Progress In Electromagnetics Research C, Vol. 99, 111–122, 2020

Truncated Circular Microstrip Ultra Wideband Antenna Exhibiting Wideband Circular Polarization

Kollannore U. Sam* **and Parambil Abdulla**

Abstract—Circular polarization is manifested by means of truncations on basic circular radiating patch with precisely designed asymmetric feed. The proposed truncated circular microstrip antenna (TCMA) yields impedance bandwidth (IBW) of 7.6 GHz, almost covering the FCC approved ultra-wideband (UWB) frequency and 3-dB axial ratio bandwidth (ARBW) of 5.05 GHz spreading over two bands, enabling the antenna to be used for multiple applications in UWB frequency range. A peak gain of 5.73 dBi is documented at 5 GHz which is within the circular polarization (CP) band. This single feed antenna is very simple to design and compact in size.

1. INTRODUCTION

Circularly polarized antenna finds major application in cellular communication, radio detection, global positioning, and other systems. Nowadays, circularly polarized planar antennas have higher acceptability because of many significant advantages over linearly polarized ones. Imperceptions towards regions of polarization, avoidance of Faraday rotation effect prevailing in the ionosphere, reduction in interference, multi-path reflections, a greater degree of tolerance in terms of orientation angle between the receiver and the transmitter are a few of them [1]. Planar antennas can be easily adopted with microwave integrated circuits owing to their compactness, light weight, and easy fabrication procedures. The purity of the circular polarization of an antenna is measured by its axial ratio. Instead of using different antennas with narrow axial ratio bandwidth, a single antenna with wide axial ratio bandwidth can be used for multiple applications. However, the maximum achievable impedance bandwidth and axial ratio bandwidth are still a bottleneck in the design of circularly polarized planar antennas to be deployed in FCC approved ultrawide frequency band (3.1–10.6 GHz).

Antennas radiate circularly polarized waves when being excited by two orthogonal field components with equal amplitude and in phase quadrature. Either coplanar waveguide (CPW) fed or microstrip fed configuration with single or dual feed arrangements can be imposed in the design of planar antenna structures. Various design techniques that are implemented to perform circular polarization in the ultra-wideband (UWB) frequency range exhibiting broad axial ratio bandwidth are reviewed. Many of the reported works that exhibit broad ARBW do not cover entire ultrawide impedance band. A CPW-fed rectangular patch antenna which can relay the entire UWB is treated in [2]. Two L-strips placed at the opposite corners of the ground so as to connect the two adjacent arms is made in. Even though the antenna covers the complete UWB, the attained ARBW is reduced to 1.952 GHz, and it is not compact. Two coplanar radiating plates with input signal fed to one of the plates and the other plate connected to the ground [3] improve the axial ratio bandwidth to 3.65 GHz, but this measurement has been done with reference taken as AR < 5 dB instead of AR < 3 dB. A single feed asymmetric radiator introduced in [4] records CP bandwidth of 2.83 GHz. CPW-fed planar antennas with various methods viz. L-shaped

Received 28 November 2019, Accepted 14 January 2020, Scheduled 30 January 2020
* Corresponding author: Kollannore U. Sam (samkoll.mes@gmail.com).
The authors are with the Division of Electronics, School of Engineering, Cochin University of Science and Technology, Kochi-22, Kerala, India.

slot and strip [5], horizontal slit and inverted L-strip on the ground [6], L-shaped slot and partial ground plane with different heights on either side of the feed line [7] are adopted to improve the ARBW. A CPW-fed planar antenna having quadrilateral shaped radiating copper and an asymmetric ground plane is illustrated in [8]. Wide impedance bandwidth is attained by inserting a step-impedance resonator in the central feed line. This work reflects a fair ARBW of 4.67 GHz. A quasi self-complementary structure and a stepped stub in the ground plane could only produce a CP bandwidth of 1.6 GHz [9]. Shorting loads are added on the patch to improve the ARBW in [10]. An antenna with an L-shaped feed line and a circular aperture with perturbation slots are introduced in [11] to expand the CP band. Many of the works based on slot antennas could not handle the entire 10-dB impedance bandwidth specified by UWB. Nevertheless, their axial ratio bandwidth covers 50% of the band except for [12] where a smooth bent feed line is introduced to attain wide CP operation (ARBW = 4.8 GHz). This antenna has a moderate gain ranging from 0.81 dBi to 3.56 dBi. Few papers which can handle the entire UWB band [13–16] could exhibit AR bandwidth of maximum 2.6 GHz. An asymmetric hexagonal shape-based slot antenna with asymmetric feed reported in [17] records an ARBW of 4.4 GHz with peak gain less than 4 dBi. A microstrip asymmetric slot antenna with asymmetric feed combined with several cuts integrated both on the slot and feed is discussed in [18]. This antenna produces an ARBW of 7.3 GHz out of which 6.7 GHz lies in the UWB and has a peak gain of 4.1 dBi. The structure of this antenna is very complex, and it requires 70 dimensional variables to be carefully designed. Spiral antenna with integrated tapered microstrip balun [19] and the one with circular cavity placed underneath as a reflector [20] enormously increases the design complexities. Dual feed configuration can also be adopted for meeting the requisite criteria of circular polarization. A dual feed system with L-shaped strips and modified ground [21] exhibiting CP of 5.06 GHz could acquire impedance band from 1.4 to 9.6 GHz with a peak gain of 3.8 dBi only. Another work proposed in [22] displays an ARBW of 2.15 GHz. Even though the dual feed arrangements reported in [23, 24] satisfy the impedance bandwidth specified for UWB band, they could sketch ARBWs of 4 GHz and 3.22 GHz respectively with a moderate gain around 3 dBi.

The rationale behind devising this proposed antenna is that all the reported single feed microstrip UWB patch antennas that claim to exhibit broad impedance bandwidth (IBW) and wide axial ratio bandwidth (ARBW) do not even attain 75% fractional ARBW covering the UWB range. Besides, their structures are not as simple as they report. One of the main drawbacks of slot antennas is that they suffer from reduced gain. The dual feed technique undergoes design complexity and mutual coupling between the two feed arrangements. Hence, in this paper, a very simple and compact single feed microstrip antenna designed for UWB applications is developed and presented. The proposed truncated circular microstrip ultra wideband antenna (TCMA) is simple in the sense that it is based on a basic circular radiating patch having explicit equations for its design, and it requires only 12 parameters for its design. The structure is compact with a dimension of $37 \times 33 \times 1.6$ mm. A modified partial ground plane is utilized to improve the frequency response of circular radiator so as to achieve an IBW of 7.6 GHz. Dissimilar truncations are deployed on either side of the radiator along with the asymmetric feed develop circular polarization producing an ARBW of 5.05 GHz. The antenna showcases a measured fractional IBW and ARBW of 105.5% and 85.8%, respectively.

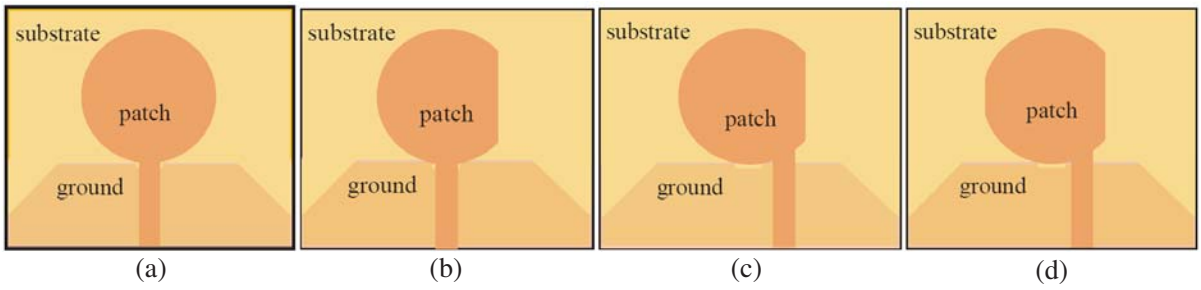

Figure 1. Geometrical evolution of the proposed antenna (TCMA) (a) circular patch with the modified partial ground, (b) circular patch with single truncation, (c) patch with asymmetric feed line and (d) TCMA with dual truncation.

2. ANTENNA CONFIGURATION AND DESIGN PROCEDURES

The proposed truncated circular microstrip antenna (TCMA) is shaped to operate in UWB frequencies specified by FCC. The geometrical evolution of TCMA is shown in Figure 1. TCMA comprises a basic circular shape radiator of radius a printed on a $37 \times 33\,\text{mm}^2$ FR-4 epoxy substrate having relative dielectric constant ε_r of 4.4, height h of 1.6 mm, and loss tangent $\tan\delta$ of 0.02. The thickness t of the patch and ground are 0.035 mm. The initial design of TCMA is based on the design formula for radius a of a circular microstrip antenna as given in Eqs. (1) and (2) [25].

$$\text{Radius,} \quad a = \frac{F}{\left[1 + \dfrac{2h}{\pi\varepsilon_r F}\left[l_n\left(\dfrac{\pi F}{2h}\right) + 1.7726\right]\right]^{1/2}} \tag{1}$$

$$\text{where,} \quad F = \frac{8.791 \times 10^9}{f_r\sqrt{\varepsilon_r}} \tag{2}$$

The signal feed line is composed of a $50\,\Omega$ microstrip line. A partial ground plane of length gl and width gw, with triangular beveling on both the sides of the ground is introduced to enhance the impedance bandwidth. A small rectangular slot is placed at the upper edge of the partial ground plane where the circular patch is likely to graze the ground apparently. This is to boost impedance matching and to exhibit a broadband response. The radiating surface of the proposed antenna is truncated to initiate circular polarization. The formula for quality factor and percentage of perturbation (3, 4) is utilized to deduce the design equation for the length of perturbation of a circular patch (5) [26]. The equation for finding the length of perturbation of a circular patch is attempted here to find the length of truncation of circular microstrip patch antenna which is schematically shown in Figure 2.

$$\text{Unloaded Quality factor,} \quad Q_0 = \frac{c\sqrt{\varepsilon_r}}{4f_0 h} \tag{3}$$

$$\text{Percentage of perturbation,} \quad \frac{\Delta_S}{s} = \frac{1}{1.84118 \times Q_0} \tag{4}$$

$$\text{Length of perturbation,} \quad l = a\sqrt{\frac{\pi}{2}}\sqrt{\frac{\Delta_S}{s}} \tag{5}$$

Now the area of perturbation is equated with the area of truncated minor segment circle.

$$2l^2 = A = a^2 \arccos\left(\frac{a-h}{h}\right) - (a-h)\sqrt{2ah - h^2} \tag{6}$$

where a is the radius of the patch, and h is the minor segment height.

Minor segment height h is resolved from Eq. (6) using the bisection method. Now the length of truncation, T, is calculated upon proper substitution of Eq. (7).

$$a^2 = \left(\frac{T}{2}\right)^2 + (a-h)^2; \quad T = 2\sqrt{2ah - h^2} \tag{7}$$

Thus the truncation $T1$ having length T is placed in $+y$ direction at a distance $d1$ from the centre of the radiating surface. The feed line is asymmetrically placed with an offset of distance $d3$ from the centre of the circular patch in the $+x$ direction. A smaller truncation $T2$ is placed in the $+y$ direction at a distance $d2$ from the centre of the patch for maintaining a stable circular polarization. An additional 1° tilt ($\theta = 1^\circ$; not shown in Figure 3) in a counter-clockwise direction is given to the smaller truncation ($T2$) in order to fine-tune the axial ratio bandwidth. The geometrical parameters of the proposed antenna for maximum axial ratio bandwidth with improved performance are labeled in Figure 3, and the same is listed in Table 1. The figure and table depict that there are only a few parameters and no complicated shapes. Hence, the structure is simple to design. All the dimensions are critical for producing wide ARBW. The fabricated prototype of TCMA is shown in Figure 4.

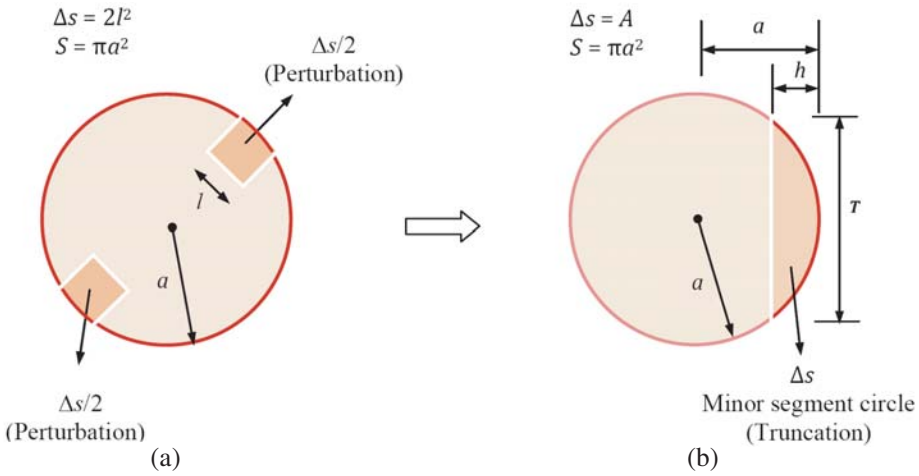

Figure 2. (a) Perturbations on a circular patch and (b) Truncation on a circular patch.

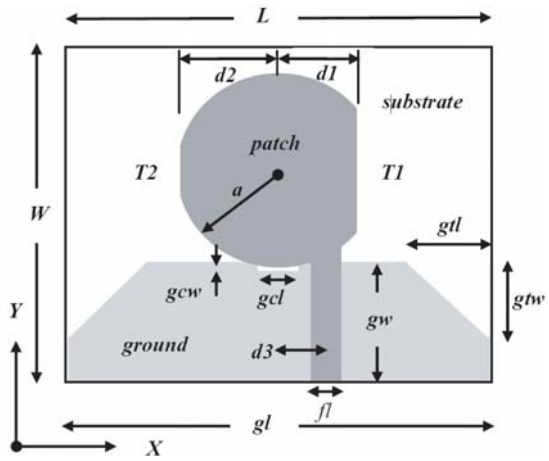

Figure 3. The geometrical layout of TCMA.

Table 1. Geometrical parameters of the proposed antenna.

Parameter	Value	Parameter	Value
L	37 mm	gtl	5.8 mm
W	33 mm	gtw	6.1 mm
gl	37 mm	gcl	3 mm
gw	11 mm	gcw	0.2 mm
a	9 mm	$d1$	6.4 mm
fl	2.1 mm	$d2$	8.8 mm
θ	1 degree	$d3$	3.4 mm

3. RESULTS AND DISCUSSION

The proposed TCMA has been designed and simulated using Finite Integral Technique (FIT) based CST Microwave Studio simulation software, fabricated using etching process, and measured using Network Analyzer ENA (E 5071C).

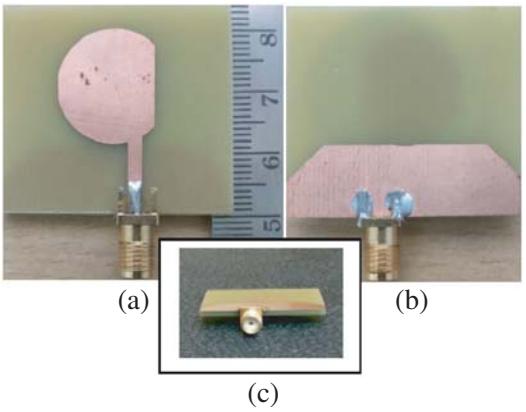

Figure 4. The fabricated prototype of the TCMA. (a) Top view. (b) Bottom view and (c) Profile view.

3.1. Return Loss

Simulated return loss plotted in Figure 5 describes that the antenna has an impedance bandwidth spreading from 3.3 GHz to 12 GHz almost roofing the frequencies of UWB (3.1–10.6 GHz) and resonating at 4.06 GHz and 10.7 GHz. The measured result displays a radiating band from 3.4 GHz to 11 GHz with a fractional bandwidth of 105.5%. The graph shows an upward displacement of only 0.14 GHz in the first resonance frequency. Variation of return loss in the upper operating frequency range is suspected to be attributed from the anticipated variations on the substrate permittivity at high frequencies and also may be due to systematic errors during measurement.

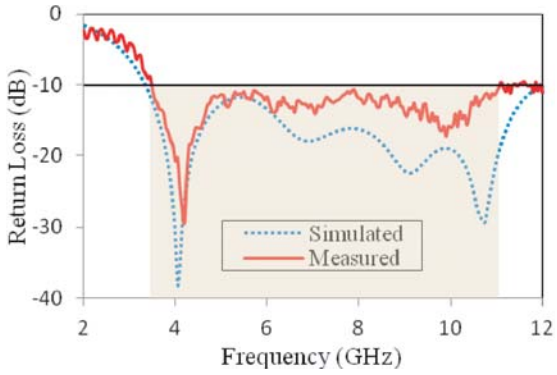

Figure 5. Simulated and measured return loss plots.

From the parametric traces drawn in Figure 6(a), it is evident that the lower frequency of resonance solely depends on the patch area. The diameter of the radiating patch is almost equal to $\lambda/4$ at the first resonating frequency. Increasing the radius of TCMA lowers the first resonant frequency. The radius of the proposed patch is legitimized to ascertain maximum axial ratio bandwidth. Figure 6(b) reveals that the effect of feed offset distance $d3$ improves impedance matching.

3.2. Axial Ratio

The requisite orthogonal modes to manifest circular polarization are developed by making truncations to either side of the radiating patch and by shifting the feed line towards the major truncation thus making the whole patch an asymmetric one.

The key geometrical parameters that significantly affect circular polarization are the distance to the truncations $d1$ and $d2$ and the asymmetric feed offset distance $d3$. Figure 7 depicts the variation of

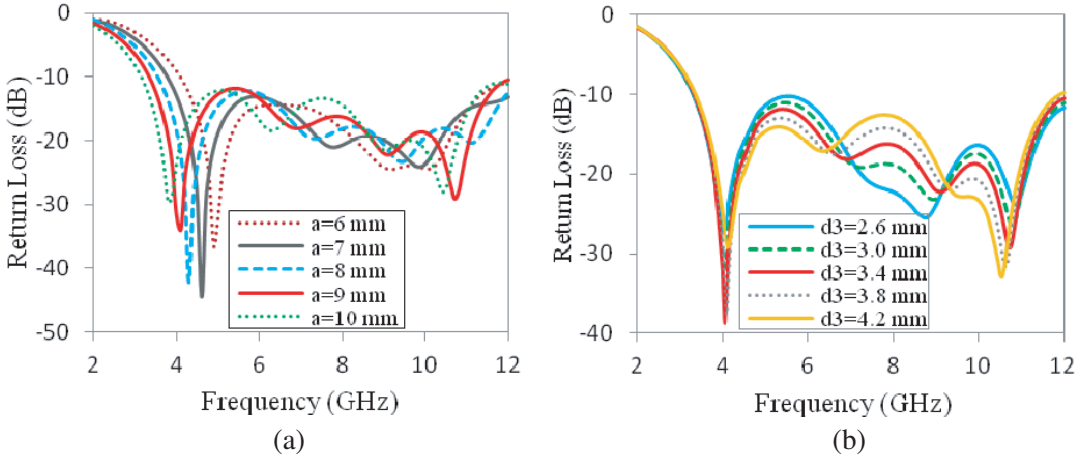

Figure 6. Parametric measurements on return loss (a) variation with patch radius and (b) variation with feed offset distance $d3$.

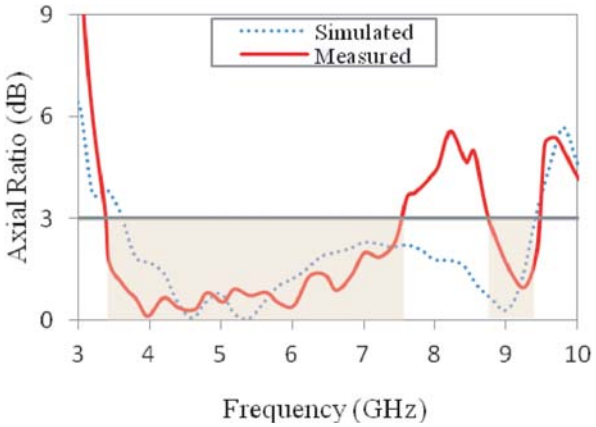

Figure 7. Simulated and measured axial ratio plots.

the axial ratio over the entire CP band. The antenna has been designed to exhibit CP from 3.6 GHz to 9.45 GHz which is self-explanatory from the simulated plot. But minor disparities are seen in the measured readings. Measured values resemble the simulated ones within the impedance bandwidth except in 7.6–8.65 GHz, thereby exhibiting circular polarization in two bands viz. 3.4–7.6 GHz (band I) and 8.65–9.5 GHz (band II), achieving an axial ratio bandwidth of 4.2 GHz and 0.85 GHz with fractional axial ratio bandwidths of 76.4% and 9.4%, respectively. A minimum value of 0.13 dB axial ratio is observed at 3.98 GHz around which the patch resonates. The deviation of the measured values from the simulated ones may be due to fabrication inaccuracies along the truncation $T1$ and asymmetric positioning of the feed line. This is because a minor misplacement of truncation $T1$ (or the distance $d1$) and the feed line offset distance $d3$ has a huge effect on axial ratio within the frequency band 7.5–9 GHz which is justified in Figure 8(a) and Figure 8(b). Also, since the connector solders and the unused ground terminals of the SMA connector are close to truncation $T1$, spurious radiations may adversely affect the measured readings.

Parametric analysis is performed to probe the variations on axial ratio with respect to those key parameters. Figure 8(a) depicts the variations of axial ratio with changing positions of truncation $T1$ under the condition that there is no truncation $T2$, and the feed line is placed centrally ($d3 = 0$). Signs of several narrowband circular polarizations are reflected by the introduction of truncation $T1$ having length T at distance $d1$ away from the centre of the circular radiating surface in the $+x$ direction. This has happened by the effect of two resonant frequencies by virtue of two different diameters in the x

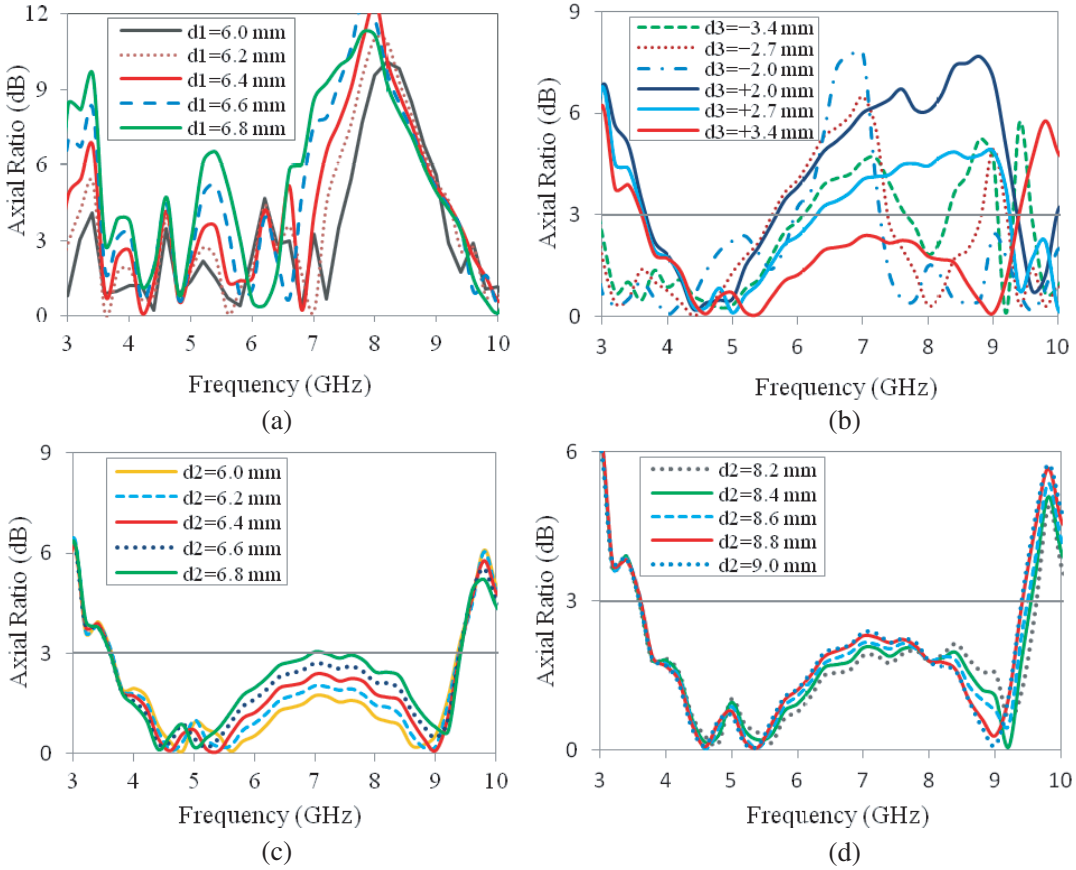

Figure 8. Parametric analysis on axial ratio (a) Effect of placement of $T1$; without $T2$ and feed offset. (b) Effect of placement of asymmetric feed; without $T2$ and $d1 = 6.4\,\text{mm}$. (c) Effect of placement of truncation $T1$; without $T2$ and $d3 = 3.4\,\text{mm}$ and (d) Effect of placement of $T2$; $d1 = 6.4\,\text{mm}$ and $d3 = 3.4\,\text{mm}$.

and y directions, with a quadrature-phase difference between the two. Figure 8(a) also reveals that the average value of axial ratio shifts down as the length of truncation $T1$ is increased till it reaches the designed value or as the distance $d1$ is decreased till $d1 = 6.4\,\text{mm}$ along the $+x$ direction (where axial ratio reads the minimum value of 0.097 dB at 4.2 GHz). Afterwards, the value of the axial ratio climbs up. Fixing $d1 = 6.4\,\text{mm}$, parametric analysis is carried out with the feed line offset distance $d3$ varying in both $+x$ and $-x$ directions without having truncation $T2$ (Figure 8(b)). The chart exposes the fact that shifting the feed line in $+x$ direction towards the truncation $T1$ has wider control in the frequency band (4.5–9.5 GHz) than shifting the feed line in the $-x$ direction. The placement of the feed line has been done accordingly. Comparing the traces in Figures 8(a) and 8(b), it is observed that by providing truncation on one side of the radiating patch along with asymmetric feed line, the average value of axial ratio has been pulled down thereby increasing the purity of circular polarization.

Keeping the feed line offset distance $d3 = 3.4\,\text{mm}$, a parametric study on axial ratio with various values of $d1$ is carried out. Figure 8(c) conveys that the position of truncation $T1$ and feed line has a pivotal role in exhibiting wideband circular polarization. Further increase in the purity of circular polarization between 8 GHz and 9 GHz is manifested by providing a small but sensitive truncation at the other side of the radiating patch at distance $d2$ from the centre of the radiating patch (Figure 8(d)). The average values of the axial ratio of the plots are seen to be again reduced. The placement of truncation $T2$ improves the stability and purity of CP without heavily sacrificing the ARBW. The enhancement in CP band compared to the earlier reported designs is achieved by means of the microstrip asymmetric feed and the dissimilar truncations on the patch.

3.3. Sense of Polarization

To assimilate the sense of polarization, investigations on the surface current distributions on the antenna at 6 GHz (representing the band I) and 9 GHz (representing the band II) are carried out. Surface current pattern diagrams (a) to (d) of Figure 9 and Figure 10 depict the surface current distribution at 0°, 90°, 180°, and 270° at 6 GHz and 9 GHz, respectively. It is evident that the direction of the surface current vector rotates in the clockwise direction, and hence TCMA exhibits LHCP in the $+z$ direction in both the bands.

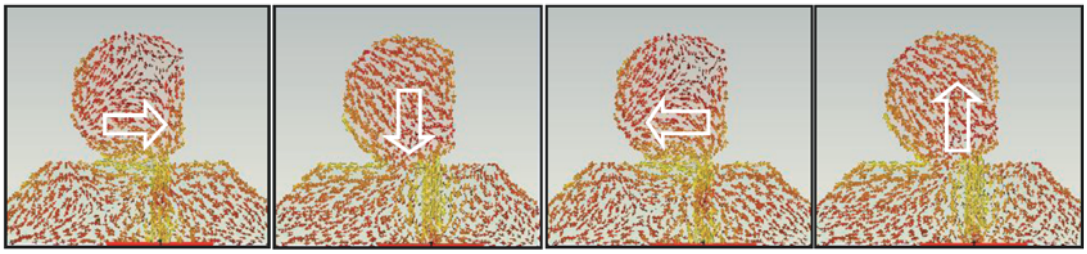

Figure 9. Surface current distribution at 6 GHz (a) Phase = 0°, (b) Phase = 90°, (c) Phase = 180° and (d) Phase = 270°.

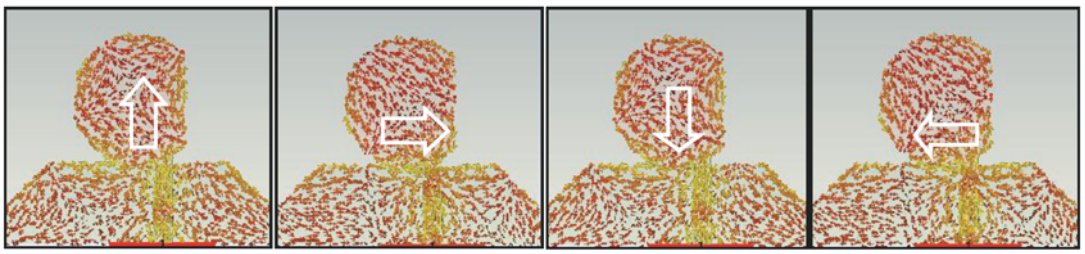

Figure 10. Surface current distribution at 9 GHz (a) Phase = 0°, (b) Phase = 90°, (c) Phase = 180° and (d) Phase = 270°.

3.4. Gain

Various traces of antenna gain along the entire frequency band are shown in Figure 11. The simulated gain varies from 1.70 dB to 5.01 dB in the operating frequency range with a peak gain of 5.01 dB at 9.5 GHz. The gain of the proposed antenna is measured using a linear horn antenna as a reference, and hence the gain trace is named as G_{dBiL}. The peak value of G_{dBiL} is 3.6 dB and is attained at 7 GHz. The measured gain, G_{dBiL}, is converted to G_{dBiC} (gain of the circularly polarized antenna) by adding 3 dB to the values of G_{dBiL} of Eq. (8) and is plotted. Another variation of G_{dBiC} is by introducing a correction factor G_{cf}, wherein the axial ratio (AR) of the antenna under test is taken into account (9, 10) [27].

$$G_{dBiC} = G_{dBiL} + 3 \tag{8}$$

$$G_{cf} = 20\log_{10}\left[0.5(1 + 10^{(-AR/20)}\right] \tag{9}$$

$$G_{dBiC} = G_{dBiL} + G_{cf} + 3 \tag{10}$$

The above two modified gain traces are plotted along with the measured and simulated ones in Figure 11. It is evident that better results than the simulated values are obtained with the modified gain, G_{dBiC}, with a peak value of 5.73 dB at 5 GHz, which lies within the broad circularly polarized band (band I). Also, the TCMA produces a positive gain throughout the entire 10-dB impedance band.

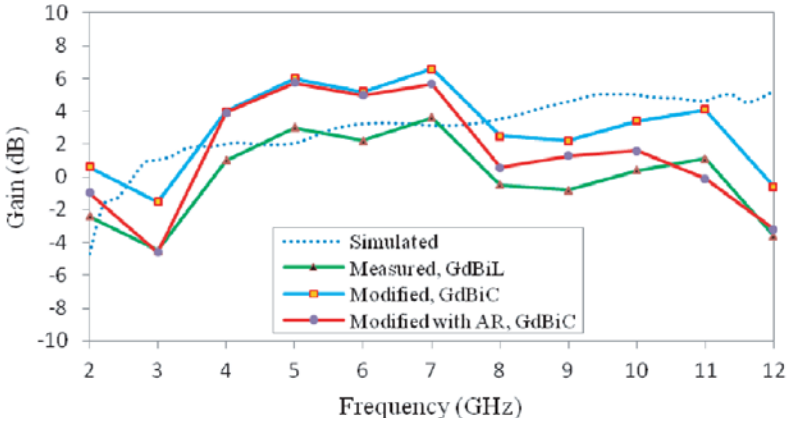

Figure 11. Simulated, measured and modified gain plots.

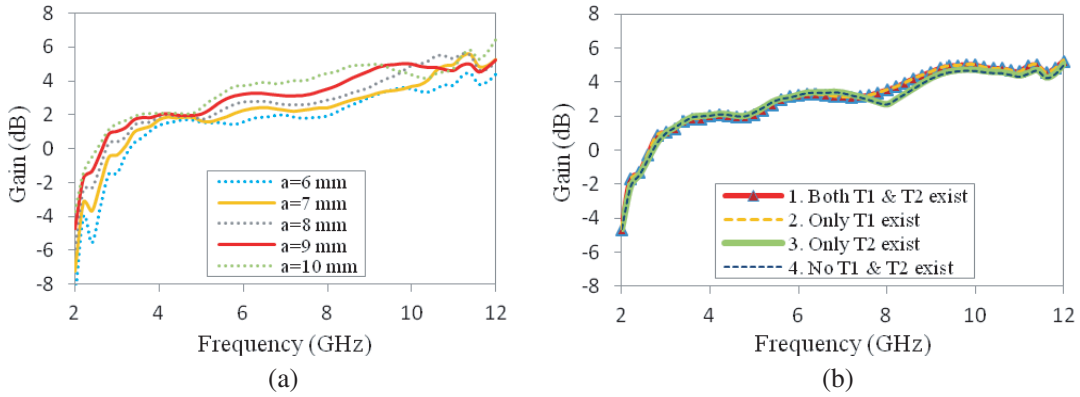

Figure 12. Parametric analysis on antenna gain (a) for different values of patch radius a and (b) with different combinations of truncations $T1$ and $T2$.

The parametric analysis performed on the antenna gain with the radius of the patch, keeping all other parameters intact, shows that the gain increases with increasing radius of the circular patch up to around 10 GHz (Figure 12(a)). Analysis on the effect of truncations on the gain of the antenna (Figure 12(b)) affirms that the antenna holding both truncations $T1$ & $T2$ and the one with only the larger truncation $T1$ have the same gain (since traces 1 and 2 overlap). Also, the antenna without holding any truncations $T1$ and $T2$ and the one with only the smaller truncation $T2$ have the same gain (since traces 3 and 4 overlap). Moreover, the antenna holding both the truncations $T1$ & $T2$ or with only the larger truncation $T1$ exhibits almost equal gain to that of antenna without holding any truncations $T1$ and $T2$ or with only smaller truncation $T2$ in the lower frequency range (up to 6.5 GHz) and precisely more gain for higher frequencies except at the mid-frequency range where its gain is slightly less. The above information conveys that the major truncation $T1$ will never degrade the gain of the antenna but to increase it in the higher frequencies except in a short mid-band range of 900 MHz.

3.5. Radiation Patterns

Normalized LHCP and RHCP radiation patterns in YZ plane and XZ plane at 3.5 GHz, 5.5 GHz, 7.2 GHz (representing CP band I), and 9.3 GHz (representing CP band II) are plotted in Figure 13.

Simulated and measured readings evidently manifest the presence of left hand circularly polarized radiation in the $+z$ axis. The antenna possesses a minimum 10 dB isolation at $\theta = 0$, except in YZ plane in the second CP band. Also, the isolation improves towards lower frequencies. The tilt in the

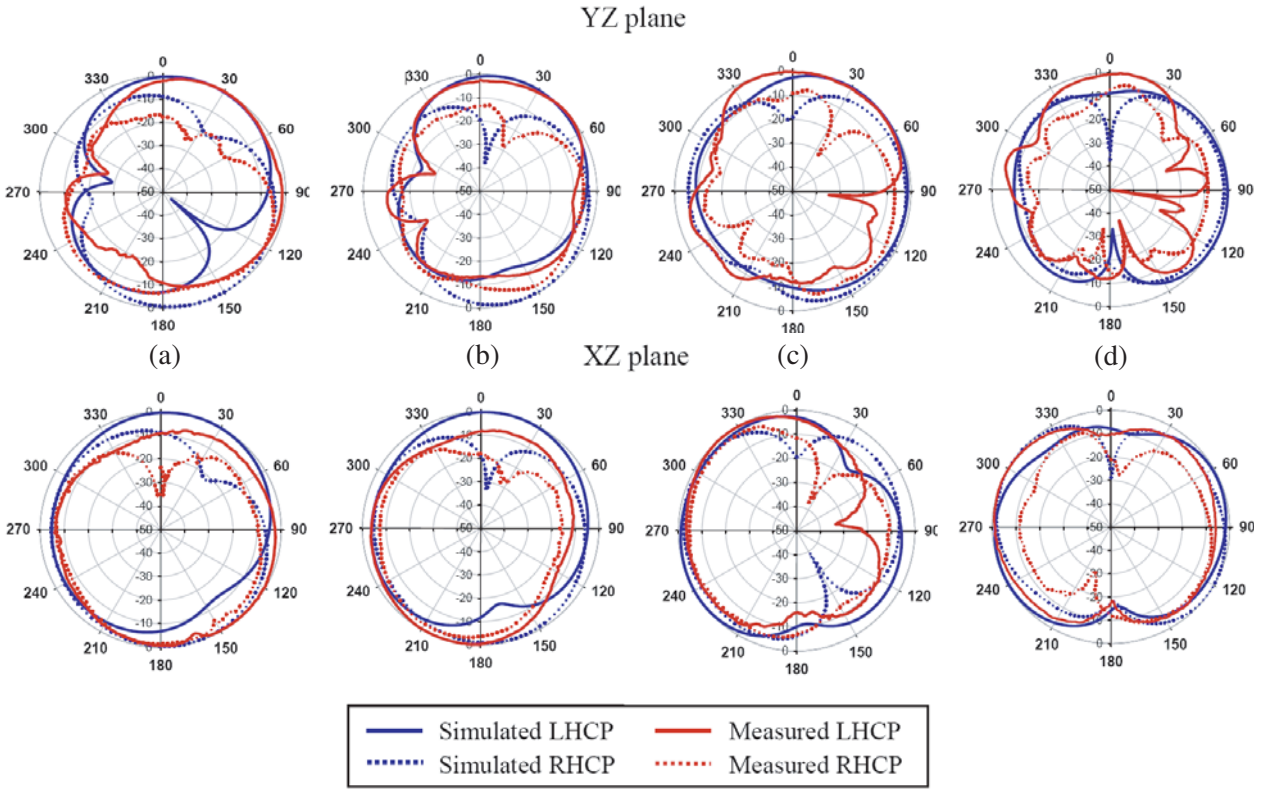

Figure 13. LHCP and RHCP radiation patterns in *YZ* plane and *XZ* plane at (a) 3.5 GHz, (b) 5.5 GHz, (c) 7.2 GHz and (d) 9.3 GHz.

Table 2. Comparison of reported broadband CP antennas with the proposed work.

Ref.	Substrate	IBW	ARBW	Peak gain
[2]	FR4: 60 × 60 × 0.8 mm	2.67–13 GHz	1.952 GHz 4.993–6.945 GHz (32.2%)	4.2 dBi
[3]	All metal: 32 × 12.5 × 7 mm	2.1–10.1 GHz	3.65 GHz 4.1–7.75 GHz (61.6%)	3.38 dBi
[4]	FR4: 28 × 29 × 1.6 mm	2.98–10.93 GHz	2.83 GHz 7.18–10.01 GHz (33%)	Not mentioned
[5]	Rogers RO4003: 20 × 20 × 0.813 mm	4.8–7.2 GHz	1.95 GHz 5.15–7.1 GHz (33%)	3.6 dBi
[6]	FR4: 25 × 24 × 1 mm	4.8–8.8 GHz	3.375 GHz 5.375–8.75 GHz (47.8%)	3.4 dB
[7]	FR4: 50 × 50×0.8 mm	2.15–6.97 GHz	3.9 GHz 3.1–7 GHz (71%)	5 dBi
[8]	FR4: 30 × 25 × 0.8 mm	3.1–17.5 GHz	4.67 GHz 5.91–10.58 GHz (56.64%)	5.67 dBi
This work	FR4: 37 × 33 × 1.6 mm	3.4–11 GHz	5.05 GHz 3.4–7.6 GHz (76.4%) and 8.65–9.5 GHz (9.4%)	5.73 dBi

radiation patterns is possibly due to the asymmetric configuration of the radiating patch and microstrip feed line.

The results of the proposed work are compared with similar reported planar antennas which make use of single feed configuration. Table 2 conveys the fact that this work deploying single asymmetric feed mechanism exhibits broad impedance bandwidth which almost covers the entire UWB frequency range (short of only 0.3 GHz) and exhibits wide axial ratio bandwidth compared to the other reported works with a fair gain in the entire passband.

4. CONCLUSION

This paper has presented an asymmetric single feed circularly polarized microstrip antenna with wide axial ratio bandwidth for UWB applications. The structure is very simple to design with only 12 dimensional parameters and compact in size. TCMA radiates signal from 3.4 GHz to 11 GHz. Asymmetrical features introduced in the antenna structure regulate the magnitude and phase of the orthogonal E-field components, which affect the value of axial ratio, and it leads to left-hand circular polarization. Circular polarization is observed as two bands from 3.4 GHz to 7.6 GHz (band I–76.4%) and from 8.65 GHz to 9.5 GHz (band II–9.4%) thus providing a total axial ratio bandwidth of 5.05 GHz (85.8%). TCMA offers adequate gain throughout the impedance bandwidth and decently good gain in the CP band with a peak gain of 5.73 dBi at 5 GHz. The proposed antenna would be a good candidate for UWB applications.

REFERENCES

1. Gao, S., Q. Luo, and F. Zhu, *Circularly Polarized Antennas*, John Wiley & Sons, 2013.
2. Pourahmadazar, J., Ch. Ghobadi, J. Nourinia, N. Felegari, and H. Shirzad, "Broadband CPW-fed circularly polarized square slot antenna with inverted L-strips for UWB Applications," *IEEE Antennas and Wireless Propagation Letters*, Vol. 10, 369–372, Apr. 2011.
3. Tsai, C. L., "A coplanar-strip dipole antenna for broad-band circular polarization operation," *Progress In Electromagnetics Research*, Vol. 121, 141–157, Oct. 2011.
4. Rahim, S. A., Sh. Danesh, U. A. Okonkwo, M. Sabran, and M. Khalily, "UWB monopole antenna with circular polarization," *Microwave and Optical Technology Letters*, Vol. 54, No. 4, 949–953, Apr. 2012.
5. Ahdi Rezaeieh, S., A. Abbosh, and M. A. Antoniades, "Compact CPW-fed planar monopole antenna with wide circular polarization bandwidth," *IEEE Antennas and Wireless Propagation Letters*, Vol. 12, 1295–1298, Oct. 2013.
6. Chen, Q., H. Zhang, L. Yang, B. Xue, and X. Min, "Broadband CPW-fed circularly polarized planar monopole antenna with inverted L-strip and asymmetric ground plane for WLAN application," *Progress In Electromagnetics Research C*, Vol. 74, 91–100, May 2017.
7. Chen, T., J. Zhang, and W. Wang, "A novel CPW-fed planar monopole antenna with broadband circularly polarization," *Progress In Electromagnetics Research M*, Vol. 84, 11–20, Aug. 2019.
8. Chaudhary, P. and A. Kumar, "Compact ultra-wideband circularly polarized CPW-fed monopole antenna," *AEU-International Journal of Electronics and Communications*, Vol. 107, 137–145, 2019.
9. Gunjan, S., "Compact circularly polarized antenna with wide axial ratio bandwidth using modified quasi-self-complementary structure," *International Journal of Microwave and Wireless Technologies*, Vol. 11, No. 1, 35–40, 2019.
10. Chao, S., "A design of compact ultrawideband circularly polarized microstrip patch antenna," *IEEE Transactions on Antennas and Propagation*, Vol. 67, No. 9, 6170–6175, 2019.
11. Zhang, Y.-X., Y.-C. Jiao, H. Zhang, and Y. Gao, "A simple broadband flat-gain circularly polarized aperture antenna with multiple radiation modes," *Progress In Electromagnetics Research C*, Vol. 81, 1–10, 2018.

12. Wu, Z., G. M. Wei, X. Li, and L. Yang, "A single-layer and compact circularly polarized wideband slot antenna based on 'bent feed'," *Progress In Electromagnetics Research Letters*, Vol. 72, 39–44, 2018.
13. Chen, Q., H. L. Zheng, T. Quan, and X. Li, "Broadband CPW-fed circularly polarized antenna with equiangular tapered-shaped feedline for ultra-wideband applications," *Progress In Electromagnetics Research C*, Vol. 26, 83–95, 2012.
14. Ram Krishna, R. V. S. and R. Kumar, "Design of ultra wideband trapezoidal shape slot antenna with circular polarization," *AEU-International Journal of Electronics and Communications*, Vol. 67, 1038–1047, Jun. 2013.
15. Shokri, M., V. Rafii, S. Karamzadeh, Z. Amiri, and B. Virdee, "Miniaturised ultra-wideband circularly polarized antenna with modified ground plane," *Electronic Letters*, Vol. 50, No. 24, 1786–1788, Nov. 2014.
16. Kumar, S., K. W. Kim, H. C. Choi, S. Saxena, R. Tiwari, M. K. Khandelwal, S. K. Palaniswamy, and B. K. Kanaujia, "A low profile circularly polarized UWB antenna with integrated GSM band for wireless communication," *AEU-International Journal of Electronics and Communications*, Vol. 93, 224–232, Jun. 2018.
17. Bhanu Pratap, L., D. Kundu, and A. Mohan, "Planar microstrip-fed broadband circularly polarized antenna for UWB applications," *Microwave and Optical Technology Letters*, Vol. 58, No. 5, 1088–1093, May 2016.
18. Prakash, K. C., P. V. Vinesh, M. Mani, S. Mathew, P. Mohanan, and K. Vasudevan, "Printed circularly polarised asymmetric ultra-wideband antenna," *Progress In Electromagnetics Research M*, Vol. 74, 179–189, 2018.
19. Mao, S. G., J. C. Yeh, and S. L. Chen, "Ultra wideband circularly polarized spiral antenna using integrated balun with application to time domain target detection," *IEEE Transactions on Antennas and Propagation*, Vol. 57, No. 7, 1914–1920, Jul. 2009.
20. Tran, H. H. and T. T. Le, "Ultrawideband, high-gain, high-efficiency, circularly polarized Archimedean spiral antenna," *AEU-International Journal of Electronics and Communications*, Vol. 109, 1–7, 2019.
21. Chandu, D. S. and S. S. Karthikeyan, "A novel broadband dual circularly polarized microstrip-fed monopole antenna," *IEEE Transactions on Antennas and Propagation*, Vol. 65, No. 3, 1410–1415, Mar. 2017.
22. Khandelwal, M. K., S. Kumar, and B. K. Kanaujia, "Design, modeling and analysis of dual-feed defected ground microstrip patch antenna with wide axial ratio bandwidth," *Journal of Computational Electronics*, Vol. 17, 1019–1028, 2018.
23. Li, Z., X. Zhu, and C. Yin, "CPW-fed ultra-wideband Slot antenna with Broadband Dual Circular Polarization," *AEU-International Journal of Electronics and Communications*, Vol. 98, 191–198, Nov. 2019.
24. Birwal, A., S. Singh, B. K. Kanaujia, and S. Kumar, "CPW-fed ultra-wideband dual-sense circularly polarized slot antenna," *Progress In Electromagnetics Research C*, Vol. 94, 219–231, 2019.
25. Balanis, C. A., *Antenna Theory: Analysis and Design*, John Wiley & Sons, Inc., 2005.
26. Kumar, G. and K. P. Ray, *Broadband Microstrip Antennas*, Artech House, Norwood, MA, 2003.
27. Toh, B. Y., R. Cahill, and V. F. Fusco, "Understanding and measuring circular polarization," *IEEE Transactions on Education*, Vol. 46, No. 3, 313–318, Aug. 2003.